NANO LETTERS

pubs.acs.org/NanoLett

Letter

Long-Range Dipole−Dipole Interactions in a Plasmonic Lattice

Ashwin K. Boddeti, Jun Guan, Tyler Sentz, Xitlali Juarez, Ward Newman, Cristian Cortes, Teri W. Odom, and Zubin Jacob*

Cite This: *Nano Lett.* 2022, 22, 22−28

Read Online

ACCESS | Metrics & More | Article Recommendations | Supporting Information

ABSTRACT: Spontaneous emission of quantum emitters can be enhanced by increasing the local density of optical states, whereas engineering dipole−dipole interactions requires modifying the two-point spectral density function. Here, we experimentally demonstrate long-range dipole−dipole interactions (DDIs) mediated by surface lattice resonances in a plasmonic nanoparticle lattice. Using angle-resolved spectral measurements and fluorescence lifetime studies, we show that unique nanophotonic modes mediate long-range DDI between donor and acceptor molecules. We observe significant and persistent DDI strengths for a range of densities that map to ∼800 nm mean nearest-neighbor separation distance between donor and acceptor dipoles, a factor of ∼100 larger than free space. Our results pave the way to engineer and control long-range DDIs between an ensemble of emitters at room temperature.

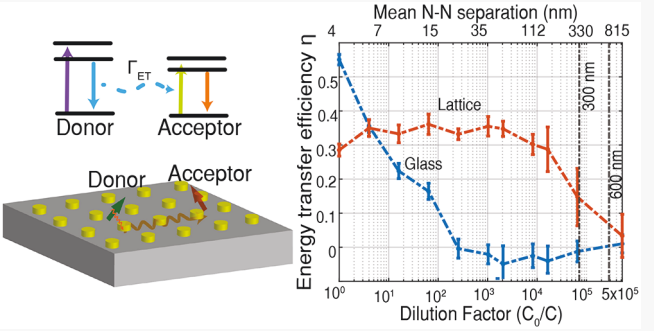

KEYWORDS: *dipole−dipole interactions, plasmonic lattice, surface lattice resonance, long-range resonance energy transfer*

Spontaneous emission and collective dipole−dipole interactions (DDIs) are two paradigms of light−matter interactions. While enhanced spontaneous emission forms the basis for devices ranging from low-threshold lasers to brighter single-photon sources,[1−4] collective DDIs offer a new tool to achieve long-range energy transfer,[5,6] superradiance,[7] quantum phases of light and matter,[8] and strongly correlated systems.[9,10] The spontaneous emission decay rate can be enhanced by modifying the local density of optical states (LDOS).[11−15] In contrast, the second paradigm of light−matter interactions, collective DDIs—between different quantum emitters sharing the common electromagnetic mode—depends on the two-point spectral density (TPSD) function. Distinct from LDOS, the TPSD function is a physical quantity that can realize dispersive interactions between quantum emitters without dissipative decay.[16−22] Physically, it captures the delocalized nature of the electromagnetic field generated by the first quantum emitter at the position of the second quantum emitter.

Long-range DDIs have been demonstrated in atomic systems coupled to waveguides,[7,23] superconducting qubits,[24] resonance energy transfer across metal thin films and cavities,[25,26] quantum phases in optical lattices,[8,27] and frameworks to engineer the isosurface in momentum space, were proposed.[28] More recently, super-Coulombic long-range interactions along material-dependent resonance angles in hyperbolic metamaterials have been explored for mediating DDIs over broad spectral ranges.[5,16,18,29] These systems, however, either rely on emitters with a spectrally narrow emission band that matches the zero-group-velocity guided modes, or have their interaction strength and range practically limited due to losses, absorption, and finite unit cell size.[5,18]

Another promising approach is to exploit the spatially extended collective modes supported by a plasmonic nanoparticle lattice. The collective lattice modes also called surface lattice resonances (SLRs) arise due to hybridization between the localized surface plasmon resonances (LSPR) in periodically arranged metal nanoparticles with diffraction orders in the plane of the array (so-called Rayleigh anomalies).[30−32] SLRs have shown to support high-quality resonances[33] and large spatial coherence.[34] They have been used to achieve strong coupling,[35,36] lasing,[37−39] magneto-optical responses,[40] room-temperature Bose−Einstein condensates,[41,42] and long-range energy transport.[43] However, spatially extended SLRs and their unique functionality for TPSD, and thus, long-range DDIs between multiple emitters have not been explored.

In this letter, we experimentally demonstrate giant collective DDIs mediated by SLRs at room temperature. The plasmonic lattice parameters are designed through rigorous numerical simulations which optimize the TPSD function, as opposed to

Received: July 21, 2021
Revised: October 3, 2021
Published: October 21, 2021

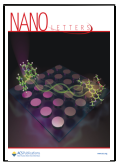

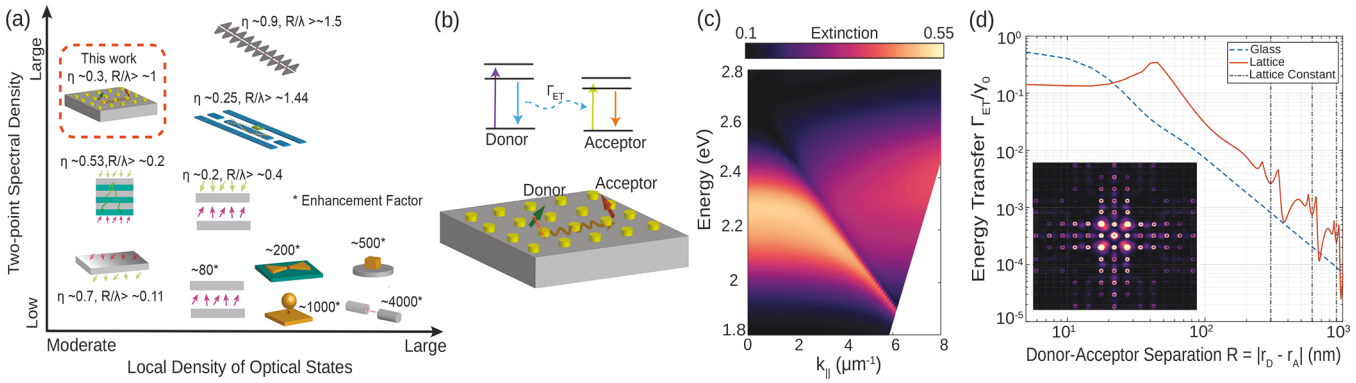

Figure 1. (a) TPSD-LDOS landscape showing the various nanophotonic environments used to demonstrate enhanced spontaneous emission and collective interactions between emitters sharing a common electromagnetic mode.[5,11,13,15,18,24−26,44,45] η is the strength of interaction, and R/λ is the effective interaction range normalized to the emission wavelength. (b) Schematic of the plasmonic lattice system used in this work. (c) Simulated angle-resolved extinction spectrum showing the dispersive modes supported by the plasmonic lattice. (d) The normalized energy-transfer rate between a donor−acceptor emitter pair separated by a distance R. The plasmonic lattice shows enhanced energy-transfer rates in comparison to the homogeneous environment—glass.

LDOS engineering. We probe the interactions through a resonance energy transfer (RET) mechanism between two different type of fluorescent dye molecules. The collective interactions between the dye molecules mediated by SLRs show significant interactions over ∼800 nm mean nearest-neighbor (N−N) separation between them. This is ∼45 times larger in comparison to conventional nondispersive homogeneous media. Our results stand out from other literature on long-range DDIs and resonance energy transfer (RET) in the following aspects: (i) We use the TPSD function to design the plasmonic lattice to enhance DDIs. This is in contrast to the conventional wisdom of enhancing LDOS. (ii) The plasmonic lattice mediates energy transfer over length scales of $R/\lambda > 1$ at room temperatures, where R is the distance between the emitters and λ is the emission wavelength. (iii) In homogeneous environments, the interaction strength scales as $1/R^6$. Here we notice strikingly different behavior on the plasmonic lattice. The interaction strength remains significant and constant up to a separation distance of ∼300 nm.

Figure 1(a) shows the LDOS-TPSD landscape with different photonic environments used either to enhance spontaneous emission[11,13,15,44] or to enhance collective DDIs.[5,18,24−26,45] LDOS only captures "local" spatial variations of the electromagnetic field in the vicinity of the emitter. In contrast, the TPSD function captures the "non-local" variations in electromagnetic modes supported by the environment. The TPSD function enhances the electromagnetic modes at the position of the second emitter due to emission from the first emitter that is spatially at a different location from the second emitter.[21,46] This indicates that dissipation (spontaneous decay) is detrimental to collective interactions. Thus, TPSD serves as a figure of merit to enhance DDIs analogous to LDOS being the figure of merit to enhance spontaneous emission. The subtle differences in dependence of DDIs and spontaneous emission on TPSD and LDOS respectively show that there exists a trade-off between LDOS and TPSD for enhancing either spontaneous emission decay rates or DDIs.[17,21,22,46,47,48]

The dipole−dipole interaction potential strength is related to the dyadic Green's function, $V_{dd}(\mathbf{r_A}, \mathbf{r_D}; \omega_D) = -(\omega_D^2/\epsilon_0 c^2)\, \mathbf{n_A}\cdot\bar{\bar{\mathbf{G}}}(r_A, r_D; \omega_D)\cdot\mathbf{n_D}$, where $\mathbf{r_A}$ and $\mathbf{r_D}$ are the positions of the two emitters, $\mathbf{n_A}$ and $\mathbf{n_D}$ are unit orientation vectors of the acceptor and donor emitters, respectively, ω_D is the radial frequency of donor emitter, ϵ_0 is the vacuum permitivitty, and c is the speed of light.[16] In DDIs, the real part of the interaction potential predicts a cooperative frequency shift, while the imaginary part predicts a cooperative decay rate between resonant emitters. It is difficult to isolate these two effects at room temperature because inhomogeneous broadening and vibrational dephasing mechanisms destroy any coherent effects between the emitters. However, it is still possible to probe DDIs at room temperature through resonance energy transfer (RET).

In RET, the excess energy due to the relaxation of the first emitter (donor) to a lower energy state is transferred to the second emitter (acceptor). This transfer is facilitated by DDIs between the donor and acceptor emitters. In homogeneous environments, RET scales as $1/R^6$, where R is limited to a few tens of nanometers. Thus, RET is an ideal probe for studying the influence of a plasmonic lattice in enhancing the strength and range of DDIs. The strength of DDI is related to the DDI potential and is depicted by the rate of energy transfer, $\Gamma_{ET}(\mathbf{r_A}, \mathbf{r_D}; \omega_D) = (2\pi/\hbar^2)|V_{dd}(\mathbf{r_A}, \mathbf{r_D}; \omega_D)|^2 f_D(\omega_D)\, \sigma_A(\omega_D)$, where $f_D(\omega_D)$ and $\sigma_A(\omega_D)$ are the emission spectra of the donor emitter and the absorption cross-sections of the acceptor emitter, respectively.[46] The energy transfer, and thus collective interactions depend on the DDI potential, V_{dd}, and the intrinsic properties of the quantum emitters. TPSD is defined as $S_{DA} = |\mathbf{n_A}\cdot\bar{\bar{\mathbf{G}}}(\mathbf{r_A}, \mathbf{r_D}; \omega_D)\cdot\mathbf{n_D}|^2$ and is quantified by evaluating the dyadic Green's function $\bar{\bar{\mathbf{G}}}(\mathbf{r_A}, \mathbf{r_D}; \omega_D)$ at the position of the second emitter, $\mathbf{r_A}$, due to the first emitter located at $\mathbf{r_D}$.[46] The TPSD in conjunction with extinction spectra of the plasmonic lattice form the basis to optimize the design parameters of the plasmonic lattice for enhanced collective interactions.

The plasmonic lattice we propose consists of silver nanopillars arranged in a periodic square lattice (300 nm periodicity) on a glass substrate (Figure 1(b)).[49] Simulated angle-resolved extinction spectra of the plasmonic lattice shown in Figure 1(c) reveal the dispersive SLR modes that mediate DDIs.[49] The strength of RET between a donor−acceptor dipole pair is estimated using the TPSD framework and is compared to a homogeneous nondispersive environment—glass. Figure 1(d) shows the distance scaling of the normalized energy-transfer rate between the donor−acceptor pair. The normalized energy-transfer rate is calculated using

https://doi.org/10.1021/acs.nanolett.1c02835
Nano Lett. 2022, 22, 22−28

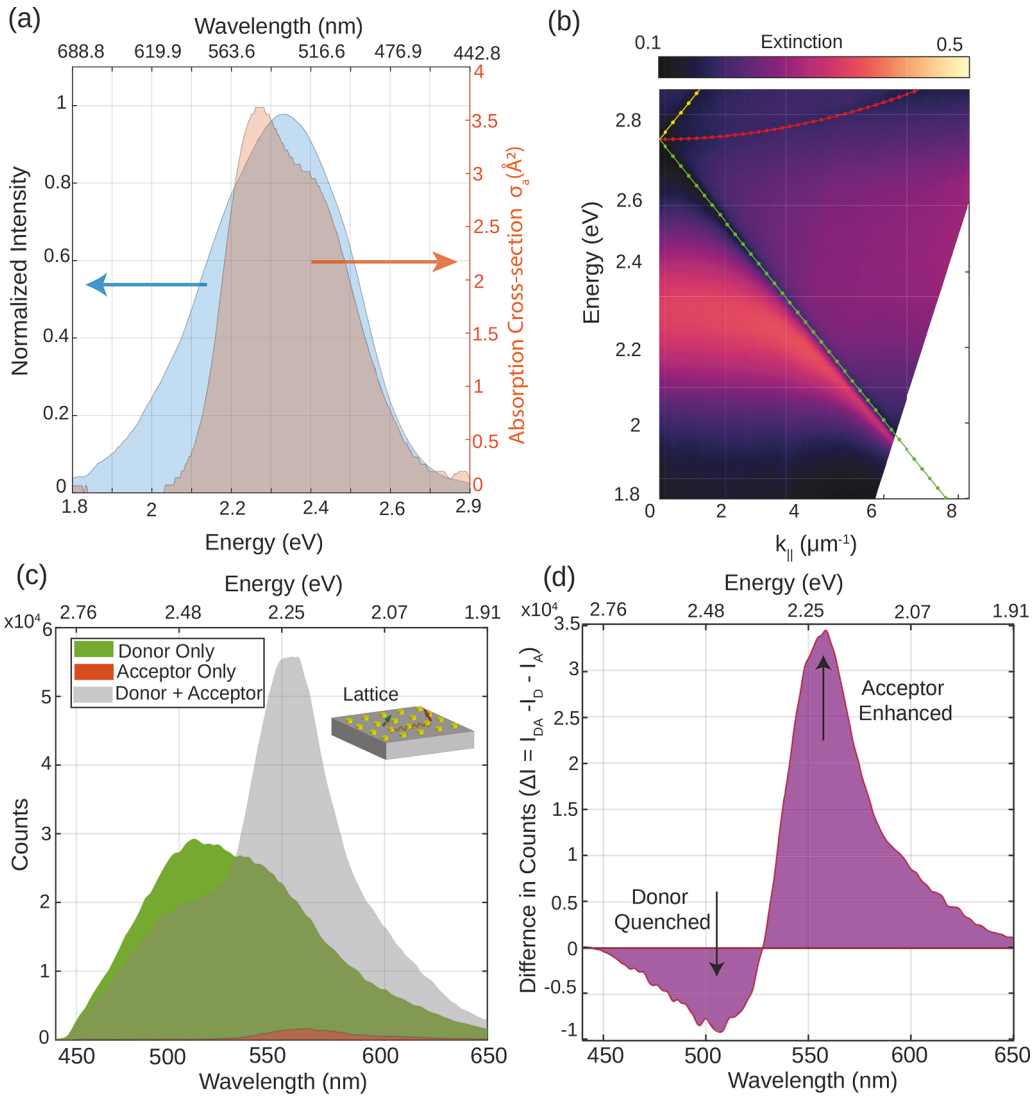

Figure 2. (a) Measured emission spectra of the Alq3 donor molecules and absorption spectra of R6G acceptor molecules. (b) Angle-resolved extinction of the plasmonic lattice using an unpolarized broadband source. (c) Fluorescence spectra of the donor only, acceptor only, and donors in the presence of acceptors on the plasmonic lattice. (d) Difference spectra on the plasmonic lattice $\Delta I = I_{DA} - I_D - I_A$ which indicates RET.

the dyadic Green's function from *ab initio* finite-difference time-domain (FDTD) simulations.[49] The inset shows the normalized electric field distribution due to the collective lattice modes supported by the lattice.

In the experiment, we use Alq3 (0.86 mM) and R6G (0.25 mM) dye molecules as donor and acceptor emitters, respectively. We embed the donor and acceptor dye molecules in PMMA polymer thin films on top of the sample.[49] Figure 2(a) shows the absorption (acceptor) and emission (donor) spectra. The spectral overlap ensures Förster-type resonance energy transfer (FRET) with an estimated Förster radius of ∼5.1 nm. Measured angle-resolved extinction spectra map the SLR modes that the plasmonic lattice supports (Figure 2(b)).[49] The two linearly dispersed branches correspond to the diffractive orders (DOs) (0, −1) (green line) and (0, 1) (yellow line) in Figure 2(b), respectively. The hyperbolically dispersed branch corresponds to the degenerate DOs (1, 0) and (−1, 0) (red line).[39,50] These dispersive modes overlap with the donor's emission and acceptor's absorption spectrum and thus help in mediating the interactions.

Steady-state spectral measurements are performed by confocally exciting the donor dye molecules with a diode laser at 402 ± 0.2 nm excitation wavelength. Figure 2(c) shows the fluorescence emission spectrum of donors only (shaded green), acceptors only (shaded orange), and a mixture of donors plus acceptors (shaded gray) measured on the plasmonic lattice. In the absence of donors, the acceptor fluorescence spectral signal is weak due to the low absorption cross-section of acceptor molecules at the excitation wavelength. Quenching at the peak emission of the donors and enhancement at the peak emission of the acceptors is observed (shaded gray) when both species of emitters are present in the PMMA polymer thin film. This is a classic signature of RET. In the presence of acceptor molecules, a donor molecule in the excited state can spontaneously decay or transfer its energy to a neighboring acceptor molecule via virtual photons. Consequent with the interaction between donor and acceptor molecules through virtual photon exchange, we observe quenching at the peak emission of the donor molecules and enhancement in emisson from acceptor molecules. The

https://doi.org/10.1021/acs.nanolett.1c02835
Nano Lett. 2022, 22, 22−28

differential spectra shown in Figure 2(d) provides evidence of this energy transfer.

Fluorescence decay lifetimes of the donor molecules are measured to probe the temporal decay dynamics and quantify the strength of DDIs. The decay lifetime of the donor molecules at their peak emission wavelength is measured using time-correlated single-photon counting technique with a narrow-band filter (520 ± 5 nm).[49] Figure 3(a,b) shows the

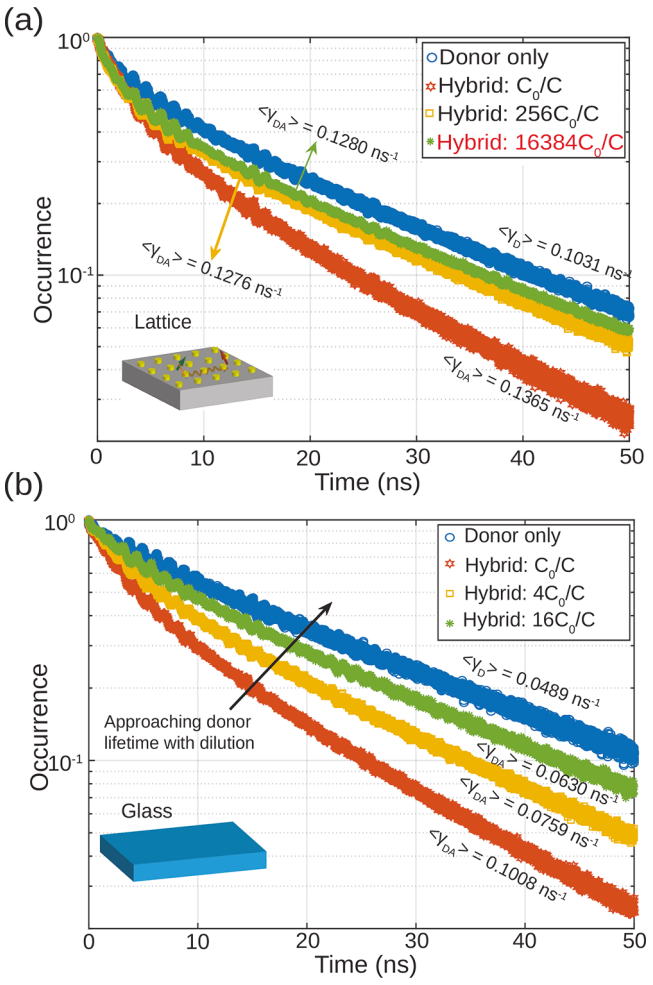

Figure 3. Measured fluorescence lifetime decay of donor molecules in the presence and absence of acceptors at various concentrations of the acceptors. (a) On the plasmonic lattice. (b) On glass.

measured decay trace of donors only (denoted as Donor) and of donors in the presence of acceptors (denoted as Hybrid) at various acceptor concentrations (denoted as a dilution factor C_0/C) on the lattice and glass substrate, respectively. Varying the acceptor concentration varies the mean N−N separation between the donor−acceptor pairs in the mixture.[49] This allows one to probe the range of DDIs mediated by SLRs. The faster decay dynamics at shorter time scales indicate the occurrence of DDIs between the donor and acceptor molecules. The measurements show that DDIs remain persistent and significant beyond C_0/C = 16 384 on the plasmonic lattice (Figure 3(a)). In contrast, the interactions appear to diminish in strength beyond C_0/C = 16 on glass (Figure 3(b)). At higher dilution factors, the fluorescence lifetime decay trace approaches that of the donor-only lifetime decay on glass. This behavior is in agreement with FRET. The persistence of interactions between the donor and acceptor molecules at very high dilution factors on the lattice clearly indicates that the plasmonic lattice significantly enhances the range of DDIs. Moreover, the interactions extend well beyond the typical FRET distances of tens of nanometers.

To elucidate the enhanced range and strength of DDIs, we estimate the mean decay rates using the harmonic mean of the measured decay trace of the donor molecules emission in the absence and presence of acceptor molecules. The harmonic mean of the measured lifetime decay trace is given as $\langle \gamma^{-1} \rangle = \int I(t)\, dt$, where $I(t)$ is the normalized lifetime decay trace.[51]

In the presence of acceptors, the total decay rate of the donor emitters, γ_{DA}, is the sum of the spontaneous decay rate of donor molecules in the absence of acceptor molecules, γ_D, and the energy-transfer rate between the donor and acceptor molecules, Γ_{ET}. Thus,

$$\Gamma_{ET} = \gamma_{DA} - \gamma_D \quad (1)$$

Figure 4(a) shows the energy-transfer rates estimated using eq 1 at different dilution factors on the plasmonic lattice and glass. Each data point corresponds to the mean value of the lifetime measurement at different spots on the sample. The uncertainty

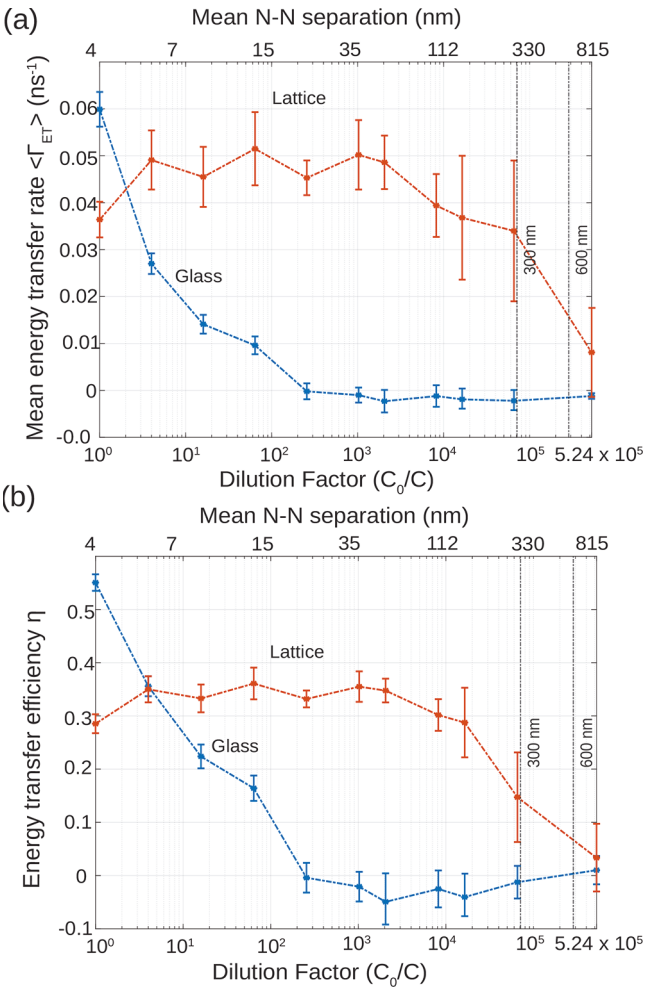

Figure 4. (a) Mean energy-transfer rates Γ_{ET} estimated from the measured fluorescence decay traces at various dilution factors on glass and the plasmonic lattice. (b) Mean energy-transfer efficiency η estimated from the mean decay rates at various dilution factors on glass and the plasmonic lattice.

https://doi.org/10.1021/acs.nanolett.1c02835
Nano Lett. 2022, 22, 22−28

in each data point denotes one standard deviation in the estimated energy-transfer rates. The energy-transfer rate between the donor and acceptor molecules on glass decreases with increase in the acceptor molecule dilution factor (blue). The top x-axis in Figure 4 shows the estimated mean N−N donor−acceptor pair separation.[49] The energy transfer between the donor−acceptor molecules vanishes at approximately 15−20 nm, corresponding to $R/\lambda \lesssim 0.04$, where R is the mean N−N donor−acceptor separation distance (20 nm) and λ is the emission wavelength (520 nm), which is the typical range of FRET.

On the contrary, the lattice mediates the interaction between the donor−acceptor molecules at orders of magnitude higher dilution factors (8000× with respect to $C_0/C = 64$ on glass). The interactions on the lattice persist beyond ∼800 nm, corresponding to $R/\lambda \gtrsim 1.54$. This clearly indicates that DDIs mediated by the SLRs significantly extend beyond the typical FRET range. The energy-transfer efficiency is estimated from the lifetime measurements as,

$$\eta = \frac{\Gamma_{ET}}{\Gamma_{ET} + \gamma_D} = 1 - \frac{\gamma_D}{\gamma_{DA}} \quad (2)$$

Figure 4(b) shows the estimated energy-transfer efficiency calculated using eq 2. The energy-transfer efficiency, η, is proportional to the strength of DDIs. We observe that this efficiency remains ∼0.33 up to a $C/C_0 \approx 16\,384$ dilution factor (∼150−200 nm mean N−N separation distance). This intriguing result is due to the modified decay lifetime of the donors (∼9.7 ns) and acceptors (∼0.87 ns) on the plasmonic lattice. The comparatively faster decay (∼11x) of acceptors effectively increases the number of acceptors available for interaction with the ensemble of donors in the excited state.[49] A first-order Taylor series expansion of eq 2 is used to estimate the uncertainty in each data point. We note that the uncertainty in η increases with the dilution factor. This observation indicates the sensitivity of RET on availability of an acceptor molecule in the vicinity of a donor molecule. As the dilution factor increases, the mean N-N separation between the donor−acceptor molecules increases. Thus, at higher dilution factors the number of acceptor molecules available to the donor molecules within the laser excitation spot varies across different regions on the sample, leading to large uncertainty in the mean decay rates and in the energy-transfer efficiencies.[49]

In summary, we have experimentally demonstrated long-range collective dipole−dipole interactions in a plasmonic lattice mediated by SLRs. The plasmonic lattice is designed on the basis of the TPSD framework. Resonance energy-transfer mechanism is used to probe and quantify the strength of DDIs in the plasmonic lattice and is compared to a nondispersive homogeneous environment—a glass substrate. The measurements show that the plasmonic lattice enhances the strength of DDIs over large donor−acceptor molecule mean nearest-neighbor separation distances of ∼800 nm. We envision that enhanced interactions will have consequential affects in creating novel light sources in quantum entanglement schemes, many-body interactions, biochemical interactions, enzyme kinetics, new classes of FRET-imaging substrates, and intercellular signaling in molecules.

■ ASSOCIATED CONTENT

Supporting Information

The Supporting Information is available free of charge at https://pubs.acs.org/doi/10.1021/acs.nanolett.1c02835.

Numerical simulations including angle-resolved extinction and computing the dyadic Green function; experimental setup; sample fabrication; polymer thin-film thickness; mean nearest-neighbor separation between donor−acceptor pairs; persistence of interactions; and mean decay rate statistics (PDF)

■ AUTHOR INFORMATION

Corresponding Author

Zubin Jacob − *Elmore Family School of Electrical and Computer Engineering, Birck Nanotechnology Center, Purdue University, West Lafayette, Indiana 47907, United States;* orcid.org/0000-0002-7009-2065; Email: zjacob@purdue.edu

Authors

Ashwin K. Boddeti − *Elmore Family School of Electrical and Computer Engineering, Birck Nanotechnology Center, Purdue University, West Lafayette, Indiana 47907, United States*

Jun Guan − *Department of Chemistry, Northwestern University, Evanston, Illinois 60208, United States;* orcid.org/0000-0001-8667-1611

Tyler Sentz − *Elmore Family School of Electrical and Computer Engineering, Birck Nanotechnology Center, Purdue University, West Lafayette, Indiana 47907, United States*

Xitlali Juarez − *Department of Materials Science and Engineering, Northwestern University, Evanston, Illinois 60208, United States*

Ward Newman − *Intel Corporation, Hillsboro, Oregon 97124, United States*

Cristian Cortes − *Center for Nanoscale Materials, Argonne National Laboratory, Lemont, Illinois 60439, United States*

Teri W. Odom − *Department of Chemistry, and Department of Materials Science and Engineering, Northwestern University, Evanston, Illinois 60208, United States;* orcid.org/0000-0002-8490-292X

Complete contact information is available at: https://pubs.acs.org/10.1021/acs.nanolett.1c02835

Notes

The authors declare no competing financial interest.

■ ACKNOWLEDGMENTS

We thank Farid Kahlor for helpful comments and discussions. We acknowledge the support of the U.S. Department of Energy, Office of Basic Sciences under DE-SC0017717, the National Science Foundation under DMR-1654676 and DMR-1904385, and the U.S. Department of Defense Vannevar Bush Faculty Fellowship under N00014-17-1-3023.

■ REFERENCES

(1) Laferriere, P.; Yeung, E.; Giner, L.; Haffouz, S.; Lapointe, J.; Aers, G. C.; Poole, P. J.; Williams, R. L.; Dalacu, D. Multiplexed single-photon source based on multiple quantum dots embedded within a single nanowire. *Nano Lett.* **2020**, *20*, 3688−3693.

(2) Harari, G.; Bandres, M. A.; Lumer, Y.; Rechtsman, M. C.; Chong, Y. D.; Khajavikhan, M.; Christodoulides, D. N.; Segev, M. Topological insulator laser: Theory. *Science* **2018**, *359*, eaar4003.

(3) Somaschi, N.; Giesz, V.; De Santis, L.; Loredo, J.; Almeida, M. P.; Hornecker, G.; Portalupi, S. L.; Grange, T.; Anton, C.; Demory, J.; et al. Near-optimal single-photon sources in the solid state. *Nat. Photonics* **2016**, *10*, 340−345.
(4) Uppu, R.; Pedersen, F. T.; Wang, Y.; Olesen, C. T.; Papon, C.; Zhou, X.; Midolo, L.; Scholz, S.; Wieck, A. D.; Ludwig, A. Scalable integrated single-photon source. *Science Advances* **2020**, *6*, DOI: 10.1126/sciadv.abc8268.
(5) Newman, W. D.; Cortes, C. L.; Afshar, A.; Cadien, K.; Meldrum, A.; Fedosejevs, R.; Jacob, Z. Observation of long-range dipole-dipole interactions in hyperbolic metamaterials. *Science Advances* **2018**, *4*, eaar5278.
(6) Deshmukh, R.; Biehs, S.-A.; Khwaja, E.; Galfsky, T.; Agarwal, G. S.; Menon, V. M. Long-range resonant energy transfer using optical topological transitions in metamaterials. *ACS Photonics* **2018**, *5*, 2737−2741.
(7) Solano, P.; Barberis-Blostein, P.; Fatemi, F. K.; Orozco, L. A.; Rolston, S. L. Super-radiance reveals infinite-range dipole interactions through a nanofiber. *Nat. Commun.* **2017**, *8*, 1857−7.
(8) Landig, R.; Hruby, L.; Dogra, N.; Landini, M.; Mottl, R.; Donner, T.; Esslinger, T. Quantum phases from competing short-and long-range interactions in an optical lattice. *Nature* **2016**, *532*, 476−479.
(9) Bluvstein, D.; Omran, A.; Levine, H.; Keesling, A.; Semeghini, G.; Ebadi, S.; Wang, T. T.; Michailidis, A. A.; Maskara, N.; Ho, W. W.; et al. Controlling quantum many-body dynamics in driven Rydberg atom arrays. *Science* **2021**, *371*, 1355−1359.
(10) Osterloh, K.; Barberán, N.; Lewenstein, M. Strongly Correlated States of Ultracold Rotating Dipolar Fermi Gases. *Phys. Rev. Lett.* **2007**, *99*, 160403.
(11) Gallego, J.; Alt, W.; Macha, T.; Martinez-Dorantes, M.; Pandey, D.; Meschede, D. Strong Purcell effect on a neutral atom trapped in an open fiber cavity. *Phys. Rev. Lett.* **2018**, *121*, 173603.
(12) Wang, D.; Kelkar, H.; Martin-Cano, D.; Utikal, T.; Götzinger, S.; Sandoghdar, V. Coherent coupling of a single molecule to a scanning Fabry-Perot microcavity. *Phys. Rev. X* **2017**, *7*, 021014.
(13) Chikkaraddy, R.; De Nijs, B.; Benz, F.; Barrow, S. J.; Scherman, O. A.; Rosta, E.; Demetriadou, A.; Fox, P.; Hess, O.; Baumberg, J. J. Single-molecule strong coupling at room temperature in plasmonic nanocavities. *Nature* **2016**, *535*, 127−130.
(14) Anger, P.; Bharadwaj, P.; Novotny, L. Enhancement and quenching of single-molecule fluorescence. *Phys. Rev. Lett.* **2006**, *96*, 113002.
(15) Akselrod, G. M.; Argyropoulos, C.; Hoang, T. B.; Ciracì, C.; Fang, C.; Huang, J.; Smith, D. R.; Mikkelsen, M. H. Probing the mechanisms of large Purcell enhancement in plasmonic nanoantennas. *Nat. Photonics* **2014**, *8*, 835−840.
(16) Cortes, C. L.; Jacob, Z. Super-Coulombic atom-atom interactions in hyperbolic media. *Nat. Commun.* **2017**, *8*, 14144.
(17) Wubs, M.; Vos, W. L. Förster resonance energy transfer rate in any dielectric nanophotonic medium with weak dispersion. *New J. Phys.* **2016**, *18*, 053037.
(18) Biehs, S.-A.; Menon, V. M.; Agarwal, G. Long-range dipole-dipole interaction and anomalous Förster energy transfer across a hyperbolic metamaterial. *Phys. Rev. B: Condens. Matter Mater. Phys.* **2016**, *93*, 245439.
(19) De Torres, J.; Mivelle, M.; Moparthi, S. B.; Rigneault, H.; Van Hulst, N. F.; García-Parajo, M. F.; Margeat, E.; Wenger, J. Plasmonic nanoantennas enable forbidden forster dipole-dipole energy transfer and enhance the FRET efficiency. *Nano Lett.* **2016**, *16*, 6222−6230.
(20) El-Ganainy, R.; John, S. Resonant dipole-dipole interaction in confined and strong-coupling dielectric geometries. *New J. Phys.* **2013**, *15*, 083033.
(21) Rustomji, K.; Dubois, M.; Kuhlmey, B.; de Sterke, C. M.; Enoch, S.; Abdeddaim, R.; Wenger, J. Direct imaging of the energy-transfer enhancement between two dipoles in a photonic cavity. *Phys. Rev. X* **2019**, *9*, 011041.
(22) Rustomji, K.; Dubois, M.; Jomin, P.; Enoch, S.; Wenger, J.; de Sterke, C. M.; Abdeddaim, R. Complete Electromagnetic Dyadic Green Function Characterization in a Complex Environment−Resonant Dipole-Dipole Interaction and Cooperative Effects. *Phys. Rev. X* **2021**, *11*, 021004.
(23) Röhlsberger, R.; Schlage, K.; Sahoo, B.; Couet, S.; Rüffer, R. Collective Lamb shift in single-photon superradiance. *Science* **2010**, *328*, 1248−1251.
(24) Van Loo, A. F.; Fedorov, A.; Lalumiere, K.; Sanders, B. C.; Blais, A.; Wallraff, A. Photon-mediated interactions between distant artificial atoms. *Science* **2013**, *342*, 1494−1496.
(25) Andrew, P.; Barnes, W. L. Förster energy transfer in an optical microcavity. *Science* **2000**, *290*, 785−788.
(26) Akulov, K.; Bochman, D.; Golombek, A.; Schwartz, T. Long-Distance Resonant Energy Transfer Mediated by Hybrid Plasmonic-Photonic Modes. *J. Phys. Chem. C* **2018**, *122*, 15853−15860.
(27) Hartmann, M. J.; Brandao, F. G.; Plenio, M. B. Strongly interacting polaritons in coupled arrays of cavities. *Nat. Phys.* **2006**, *2*, 849−855.
(28) Ying, L.; Zhou, M.; Mattei, M.; Liu, B.; Campagnola, P.; Goldsmith, R. H.; Yu, Z. Extended range of dipole-dipole interactions in periodically structured photonic media. *Phys. Rev. Lett.* **2019**, *123*, 173901.
(29) Milton, G. W.; McPhedran, R. C.; Sihvola, A. The searchlight effect in hyperbolic materials. *Opt. Express* **2013**, *21*, 14926−14942.
(30) Auguié, B.; Barnes, W. L. Collective resonances in gold nanoparticle arrays. *Phys. Rev. Lett.* **2008**, *101*, 143902.
(31) Kravets, V.; Schedin, F.; Grigorenko, A. Extremely narrow plasmon resonances based on diffraction coupling of localized plasmons in arrays of metallic nanoparticles. *Phys. Rev. Lett.* **2008**, *101*, 087403.
(32) Kravets, V. G.; Kabashin, A. V.; Barnes, W. L.; Grigorenko, A. N. Plasmonic surface lattice resonances: A Review of properties and applications. *Chem. Rev.* **2018**, *118*, 5912−5951.
(33) Bin-Alam, M. S.; Reshef, O.; Mamchur, Y.; Alam, M. Z.; Carlow, G.; Upham, J.; Sullivan, B. T.; Ménard, J.-M.; Huttunen, M. J.; Boyd, R. W.; et al. Ultra-high-Q resonances in plasmonic metasurfaces. *Nat. Commun.* **2021**, *12*, 974.
(34) Shi, L.; Hakala, T. K.; Rekola, H. T.; Martikainen, J.-P.; Moerland, R. J.; Törmä, P. Spatial Coherence Properties of Organic Molecules Coupled to Plasmonic Surface Lattice Resonances in the Weak and Strong Coupling Regimes. *Phys. Rev. Lett.* **2014**, *112*, 153002.
(35) Vakevainen, A.; Moerland, R.; Rekola, H.; Eskelinen, A.-P.; Martikainen, J.-P.; Kim, D.-H.; Torma, P. Plasmonic surface lattice resonances at the strong coupling regime. *Nano Lett.* **2014**, *14*, 1721−1727.
(36) Rodriguez, S.; Rivas, J. G. Surface lattice resonances strongly coupled to Rhodamine 6G excitons: tuning the plasmon-exciton-polariton mass and composition. *Opt. Express* **2013**, *21*, 27411−27421.
(37) Hakala, T.; Rekola, H.; Väkeväinen, A.; Martikainen, J.-P.; Nečada, M.; Moilanen, A.; Törmä, P. Lasing in dark and bright modes of a finite-sized plasmonic lattice. *Nat. Commun.* **2017**, *8*, 13687.
(38) Guo, R.; Nečada, M.; Hakala, T. K.; Väkeväinen, A. I.; Törmä, P. Lasing at K Points of a Honeycomb Plasmonic Lattice. *Phys. Rev. Lett.* **2019**, *122*, 013901.
(39) Guan, J.; Sagar, L. K.; Li, R.; Wang, D.; Bappi, G.; Wang, W.; Watkins, N.; Bourgeois, M. R.; Levina, L.; Fan, F.; et al. Quantum dot-plasmon lasing with controlled polarization patterns. *ACS Nano* **2020**, *14*, 3426−3433.
(40) Kataja, M.; Hakala, T.; Julku, A.; Huttunen, M.; van Dijken, S.; Törmä, P. Surface lattice resonances and magneto-optical response in magnetic nanoparticle arrays. *Nat. Commun.* **2015**, *6*, 7072.
(41) Rodriguez, S. R. K.; Feist, J.; Verschuuren, M. A.; Garcia Vidal, F. J.; Gómez Rivas, J. Thermalization and Cooling of Plasmon-Exciton Polaritons: Towards Quantum Condensation. *Phys. Rev. Lett.* **2013**, *111*, 166802.
(42) Hakala, T. K.; Moilanen, A. J.; Väkeväinen, A. I.; Guo, R.; Martikainen, J.-P.; Daskalakis, K. S.; Rekola, H. T.; Julku, A.; Törmä,

P. Bose−Einstein condensation in a plasmonic lattice. *Nat. Phys.* **2018**, *14*, 739−744.
(43) Yadav, R. K.; Otten, M.; Wang, W.; Cortes, C. L.; Gosztola, D. J.; Wiederrecht, G. P.; Gray, S. K.; Odom, T. W.; Basu, J. K. Strongly Coupled Exciton-Surface Lattice Resonances Engineer Long-Range Energy Propagation. *Nano Lett.* **2020**, *20*, 5043−5049.
(44) Santhosh, K.; Bitton, O.; Chuntonov, L.; Haran, G. Vacuum Rabi splitting in a plasmonic cavity at the single quantum emitter limit. *Nat. Commun.* **2016**, *7*, 11823.
(45) Hood, J. D.; Goban, A.; Asenjo-Garcia, A.; Lu, M.; Yu, S.-P.; Chang, D. E.; Kimble, H. Atom-atom interactions around the band edge of a photonic crystal waveguide. *Proc. Natl. Acad. Sci. U. S. A.* **2016**, *113*, 10507−10512.
(46) Cortes, C. L.; Jacob, Z. Fundamental figures of merit for engineering Förster resonance energy transfer. *Opt. Express* **2018**, *26*, 19371−19387.
(47) Collison, R.; Pérez-Sánchez, J. B.; Du, M.; Trevino, J.; Yuen-Zhou, J.; O'Brien, S.; Menon, V. M. Purcell Effect of Plasmonic Surface Lattice Resonances and Its Influence on Energy Transfer. *ACS Photonics* **2021**, *8*, 2211−2219.
(48) Rout, S.; Koutsares, S. R.; Courtwright, D.; Mills, E.; Shorter, A.; Prayakarao, S.; Bonner, C. E.; Noginov, M. A. Effect of nanoscale dielectric environments on concentration quenching, *Nanophotonics* (2021): 000010151520210132, DOI: 10.1515/nanoph-2021-0132.
(49) See Supporting Information for details on the modeling of modes supported by the lattice, Green's function calculation, the experimental setup, sample fabrication, sample fabrication, mean nearest-neighbour separation calculation, persistence of interactions, and mean decay rate statistics.
(50) Guo, R.; Hakala, T. K.; Törmä, P. Geometry dependence of surface lattice resonances in plasmonic nanoparticle arrays. *Phys. Rev. B: Condens. Matter Mater. Phys.* **2017**, *95*, 155423.
(51) Berberan-Santos, M.; Bodunov, E.; Valeur, B. Mathematical functions for the analysis of luminescence decays with underlying distributions 1. Kohlrausch decay function (stretched exponential). *Chem. Phys.* **2005**, *315*, 171−182.

https://doi.org/10.1021/acs.nanolett.1c02835
Nano Lett. 2022, 22, 22−28